10 OCT 2000

Final Report

Approximate wall boundary conditions in the large-eddy simulation of high Reynolds number flow

Submitted by:

Parviz Moin, *Principal Investigator*
moin@stanford.edu
(650) 723-9713

Stanford University
Mechanical Engineering Department
Flow Physics and Computation Division
Stanford, CA 94305-3030

Prepared with support of Air Force Grant number F49620-97-1-0210-P00003

Approximate wall boundary conditions in the large-eddy simulation of high Reynolds number flow

Executive Summary: The near-wall regions of high Reynolds numbers turbulent flows must be modelled to treat many practical engineering and aeronautical applications. In this project we carried out and analyzed results from simulations of both attached and separated flows on coarse grids in which the near-wall regions were not resolved and were instead represented by approximate wall boundary conditions. The simulations use the dynamic Smagorinsky subgrid-scale model and a second-order finite-difference method. Typical results are found to be mixed, with acceptable results found in many cases in the core of the flow far from the walls, provided there is adequate numerical resolution, but with poorer results generally found near the wall. Deficiencies in this approach are caused in part by both inaccuracies in subgrid-scale modelling and numerical errors in the low-order finite-difference method on coarse near-wall grids, which should be taken into account when constructing models and performing large-eddy simulation on coarse grids. A promising new method for developing wall models from optimal control theory was developed which is being pursued under a new AFOSR contract.

Abbreviations: DNS – direct numerical simulation; LES – large-eddy simulation; RANS – Reynolds-averaged Navier-Stokes; SGS – subgrid-scale; TBLE – thin boundary layer equations

Nomenclature: A^+ – damping function parameter; B – log law intercept; C – dynamic coefficient for the Smagorinsky model; C_f – friction coefficient, $2\tau_w/U_\infty^2$; C_p – relative wall pressure coefficient, $2(P_w - P_o)/U_\infty^2$; h – step height; k – turbulent kinetic energy; L – inertial length scale, k/ε; $\mathcal{L}$ – residual SGS stress between test and grid filter levels; $\mathcal{M}$ – residual SGS model strain between test and grid filter levels; P – mean pressure; P_m – matching pressure at y_m; Re_h – step Reynolds number, $U_\infty h/\nu$; Re_τ – friction Reynolds number, $u_\tau \delta/\nu$; $\mathbf{S}$ – strain rate tensor; $\mathcal{T}$ – residual SGS stress at test filter level; U – mean streamwise velocity; u' – streamwise rms velocity fluctuation intensity; $\tilde{u}_j$ – velocity in the inner layer; U_∞ – free stream velocity; U_m – streamwise matching velocity at y_m; U_{mi} – matching velocity at y_m in the ith direction; u_τ – friction speed; x – streamwise coordinate; y – wall-normal coordinate; y^+ – wall-normal coordinate in wall units, yu_τ/ν; y_m – log law intercept; δ – channel half-width or boundary layer thickness; Δ – effective filter width; ε – turbulent dissipation rate; κ – von Kármán constant, inverse slope of log law; ν – kinematic coefficient of molecular viscosity; ν_s – SGS eddy viscosity; ν_t – eddy viscosity in the inner layer; τ – residual SGS stress at grid filter level; τ_w – streamwise wall stress; τ_{wi} – wall stress in the ith direction

1 Introduction

The near-wall region in high Reynolds number turbulent flow contains small vortical structures (streaks) that are dynamically important to the flow, but which have dimensions that scale with the viscous scale, making it impractical to resolve them in numerical simulations at very high Reynolds numbers. Thus there is a crucial need to approximate the overall dynamical effects of the streaks on the larger outer scales through appropriate boundary conditions without resolving the inner viscous regions. On the other hand, the need for approximate wall boundary conditions has not been so well established in separated flow regions, which do not exhibit this streak-like structure, and which behave effectively like low Reynolds numbers flows with lower resolution requirements.

In 1970 Deardorff [17], constrained by the limited computing power of his time, performed a large-eddy simulation (LES) of channel flow with no molecular viscosity on a very coarse grid. He used approximate boundary conditions, matching the second wall-normal derivatives to the log law values, and an eddy viscosity subgrid-scale (SGS) model, with which he obtained fairly poor mean flow statistics. The same near-wall resolution problem presents itself to us today, even though we have vastly greater computing power than in 1970, as we attempt to simulate more complex, high Reynolds number flows.

1.1 LES resolution issues

Current subgrid-scale models, which generally do a good job predicting unresolved turbulent dissipation, do not model unresolved stresses accurately when they are a significant fraction of the total Reynolds stress [28]. As a consequence, a proper LES must resolve all "large" turbulent scales in the flow, viz., those that contain most of the turbulent kinetic energy and Reynolds shear stress in a localized region of the flow. Another way to put this is that the grid spacing Δ should be some minimal ratio of the local inertial length scale, $L = k^{3/2}/\varepsilon$, where k is the turbulent kinetic energy and ε is the turbulent dissipation rate; this ratio has been estimated to be $\Delta/L \approx 1/10$ to obtain good results in channel flow [4]. Near walls in boundary layers the size of turbulent eddies scales roughly as the distance from the wall, limited by viscous scales, which means that well resolved LES requires grids nearly as fine as those used in direct numerical simulation (DNS). This restriction applies not only to wall-normal grid spacing but to horizontal grid spacing as well. Baggett et al. [4] estimated that the number of grid points necessary to resolve a channel flow properly with LES scales approximately as Re_τ^2. In well resolved LES of wall-bounded flow, most of the grid points are thus used in the near-wall regions. An example of this is a simulation with zonal refinement near the walls at a modest friction Reynolds number $Re_\tau = 1000$ [27], in which 70% of grid points were allocated in near-wall zones comprising only 10% of the channel width. The time step in the simulations must also be decreased accordingly with these finer grids for numerical stability.

We note that, in practice, many LES applications use fairly coarse horizontal grids —too coarse in fact to resolve the energy-containing scales accurately—, but refine the grid in the wall-normal direction to nearly DNS accuracy to "resolve" the buffer and viscous regions; we will refer to such

in both the wall-normal and horizontal directions to capture the energy-bearing scales of motion or even the variation of the mean flow in the wall-normal direction. With a zonal or unstructured mesh, one could provide a mesh for the outer flow that does capture the energy-containing scales down to a certain distance from the wall that is physically reasonable (say, within some small fraction of the boundary layer thickness) and affordable for the given computational resources. Boundary conditions on all velocity components are then specified at the location off of the wall where the grid ends.

Attempts at using such "off-wall" boundary conditions synthesized from rescaled interior flow data [7, 36, 29] have proven to be largely unsuccessful. Baggett [5] performed tests using exact near-wall flow data in a channel, obtained from a wall-resolved LES, as an off-wall boundary condition; by scrambling the phases of the data, he found that the interior flow was severely disrupted near the artificial boundary unless the relative phases and the time scales of the original flow were preserved in the boundary plane, indicating that a good deal of physical structural information is required for off-wall boundary conditions to avoid generating spurious transition regions. Jiménez & Vasco [29] found that the interior flow is very sensitive to the boundary-normal transpiration velocity; if it is incompatible in the sense of continuity from the interior flow, then large pressure and velocity fluctuations are generated. The off-wall boundary may also be generally incompatible in the sense of injecting an unphysical rate of energy into the interior flow; this may also be a problem in wall stress models. Any workable off-wall model will need to satisfy rather severe constraints like this, which makes them very difficult to construct successfully.

The usual result of applying poorly designed off-wall boundary conditions is the appearance of a strong, spurious boundary layer above the artificial boundary. The rest of the outer flow may also be affected adversely in addition because of the spurious pressure generated at the artificial boundary, which is felt everywhere in incompressible flow. Because of these problems, we will restrict our further discussion to the performance of wall stress models.

1.4 Numerical scheme

Throughout this paper we will discuss results using second-order central finite differencing on a staggered grid [23, 25] and a third-order Runge-Kutta time advancement scheme, whose numerical properties have been examined in some detail [15, 32, 20, 26]. Numerical dispersion errors are known to be high for second-order differencing, which effectively reduces the spatial resolution to about 1/3 that of spectral methods for same number of grid points in each direction [32], and in which numerical errors are probably comparable to the contributions from the SGS model [20]. However, low-order codes like these have good conservation properties, are relatively flexible for implementation in complex geometries, and are hence widely used in engineering flow applications. It is therefore of practical interest to examine their performance using LES on coarse grids with wall models. We will also only consider simulations using the standard dynamic SGS model [19, 31]. These choices, as will be seen further on, have important consequences on the wall model results.

$\kappa \approx 0.4$ is von Kármán's constant, and $B \approx 5$ is the log law intercept; or a more complicated composite formula for u_τ including the viscous and "wake" regions [16] can solved in flows featuring low Reynolds number regions (e.g., near separation). For rough walls, the value of the matching height y_m is usually offset by an effective roughness thickness [33]. These equations are generally transcendental in u_τ, but can be solved quite efficiently with a few Newton iterations. Sometimes equation (1) is applied only to the mean streamwise component of velocity in simple flows [42, 22], or an effort is made to calculate the wall stress in alignment with the full horizontal velocity [33, 11]. Because flow conditions at a height y_m affect the wall some distance downstream, one can shift U_m and τ_w either manually by an empirical amount [40] or by time averaging the matching velocity from the outer flow over roughly the diffusion time of the inner layer. This shift is seen to increase the correlation of U_m and τ_w in a priori tests of resolved flow simulations from about 30 to 50%, and slight improvements in the mean flow results have been reported [40]. Note that the level of averaging used in specifying U_m affects the calibration of log law constants in equation (1) [33]. Werner & Wengle [47] fit the instantaneous horizontal velocities to a profile comprising a power law (rather than a log law) matched to a linear near-wall segment to obtain wall stresses, which does not give significantly different wall stress predictions from the previously cited models; for the subgrid-scale eddy viscosity they also switched from a Smagorinsky model to a mixing length model near walls.

In geometrically simple flows like channel, horizontally averaged U_m can be used to set a mean τ_w, with fluctuations set equal to the near-wall velocity fluctuations [42, 22]. Wu & Squires [48] generalized this approach to complex boundaries by obtaining a steady RANS solution for the near-wall region to determine the mean wall stress and using instantaneous outer flow information to set the local fluctuations in the wall stress.

2.2 Wall stresses using thin boundary layer equations

The unsteady thin boundary layer equations (TBLE), which in general are a simplified set of partial differential equations derived from the Navier-Stokes equations, can also be used, especially in flows with large pressure gradients which require more detailed momentum balance information [8]. The governing equations for inner horizontal velocity components $\widetilde{u}_i$ $(i = 1, 3)$ are

$$\frac{\partial \widetilde{u}_i}{\partial t} + \frac{\partial (\widetilde{u}_i \widetilde{u}_j)}{\partial x_j} + \frac{\partial P_m}{\partial x_i} = \frac{\partial}{\partial y}\left[(\nu + \nu_t)\frac{\partial \widetilde{u}_i}{\partial y}\right] \tag{2}$$

with continuity

$$\widetilde{u}_2 = -\int_0^y \frac{\partial \widetilde{u}_i}{\partial x_i}\, dy' \,, \tag{3}$$

and with matching interior boundary condition $\widetilde{u}_i(y_m) = U_{mi}$ and wall boundary condition $\widetilde{u}_i(0) = 0$. In equation (2), P_m is the near-wall pressure from the outer flow, assumed to be independent of y in the inner layer. The eddy viscosity ν_t is usually modelled with an ad hoc damped mixing length prescription that approximates the linear and logarithmic regions for attached flow with reasonable

surprisingly good success under the circumstances (see Section 3.2). The cost of computing the LES of the outer flow, of course, decreases dramatically using wall stress models, since much coarser grids can be used near walls and, for explicit numerical schemes, larger time steps can be used. The precise savings one gains in computational cost depends very much on the complexity of the flow and the complexity of the wall model employed.

2.3 Subgrid-scale modelling

In the simulations we will be considering, the standard dynamic procedure is applied to the Smagorinsky [43] SGS model for the trace-free (*) part of the residual stress τ [19, 31]:

$$\tau^* = (\overline{\mathbf{u}\mathbf{u}} - \overline{\mathbf{u}}\,\overline{\mathbf{u}})^* \sim -2\nu_s\overline{\mathbf{S}} = -2C\Delta^2|\overline{\mathbf{S}}|\overline{\mathbf{S}}\,, \tag{7}$$

where $\bar{}$ denotes the filter, ν_s is the SGS eddy viscosity, C is the Smagorinsky coefficient, Δ is the effective grid width, and $\overline{\mathbf{S}}$ is the resolved strain tensor. At a coarser scale given by an additional test filter $\hat{}$, the residual stress is

$$T^* = (\widehat{\overline{\mathbf{u}}\overline{\mathbf{u}}} - \widehat{\overline{\mathbf{u}}}\,\widehat{\overline{\mathbf{u}}})^* \sim -2\hat{\nu}_s\widehat{\overline{\mathbf{S}}} = -2C\hat{\Delta}^2|\widehat{\overline{\mathbf{S}}}|\widehat{\overline{\mathbf{S}}}\,. \tag{8}$$

Test filtering equation (7) and combining with (8), assuming that C is not affected by the filtering operation, gives an algebraic expression for C in terms of test-filtered flow quantities, which is solved in a least-squares sense over tensor components and a spatial average $\langle\rangle$:

$$C \sim \langle \mathcal{L} : \mathcal{M}\rangle / \langle \mathcal{M} : \mathcal{M}\rangle\,, \tag{9}$$

where

$$\mathcal{L} \equiv (\widehat{\overline{\mathbf{u}}\overline{\mathbf{u}}} - \widehat{\overline{\mathbf{u}}}\,\widehat{\overline{\mathbf{u}}})^*\,, \quad \mathcal{M} \equiv 2(\Delta^2|\widehat{\overline{\mathbf{S}}}|\widehat{\overline{\mathbf{S}}} - \hat{\Delta}^2|\widehat{\overline{\mathbf{S}}}|\widehat{\overline{\mathbf{S}}})\,. \tag{10}$$

A more mathematically rigorous formulation of the dynamic procedure, including effects of backscatter, is provided by Ghosal & Moin [21].

In plane-parallel flows, filtering and averaging are performed only on horizontal planes parallel to the walls. When the simulation uses a refined wall-normal grid, this may be justified, since the filtering over very small wall-normal distances has little effect. This approach is not at all justified when the mesh is so coarse in the wall-normal directions that large flow variations are being averaged over. The general class of commutative filters developed by Vasilyev et al. [45], which is normally applicable to all directions in wall bounded flows, is not appropriate here for the same reason. Also the terms used to compute C in the dynamic procedure, especially strain terms involving wall-normal derivatives, cannot be determined accurately on a coarse grid near walls. We therefore recognize from the outset that the SGS model may be highly inaccurate in the near-wall region, and that improvements are clearly needed in SGS/wall modelling in this area.

When filters are much wider than energy-containing scales, as is the case on coarse near-wall meshes, one expects that the effect of large-scale spatial averaging over many turbulent eddies might correspond to a Reynolds average. In that case, one would be justified in switching from SGS

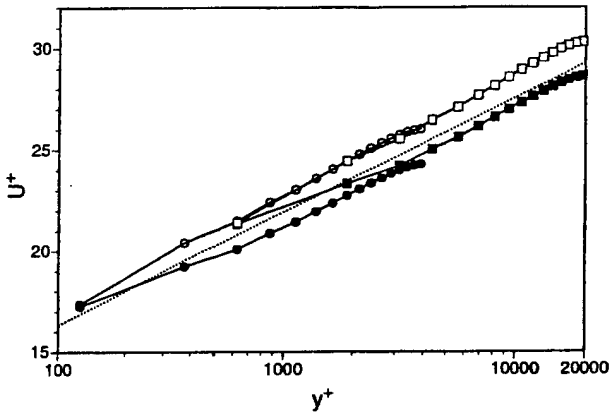

Figure 1: Mean streamwise velocity in wall units for LES with TBLE wall stress models on a 32^3 mesh at $Re_\tau = 4000$ (circles) and 20000 (squares) with (open symbols) and without (solid symbols) enhanced SGS eddy viscosity near the walls. The log law (Eq. 1) using $\kappa = 0.41$ and $B = 5.1$ is also shown (dotted line).

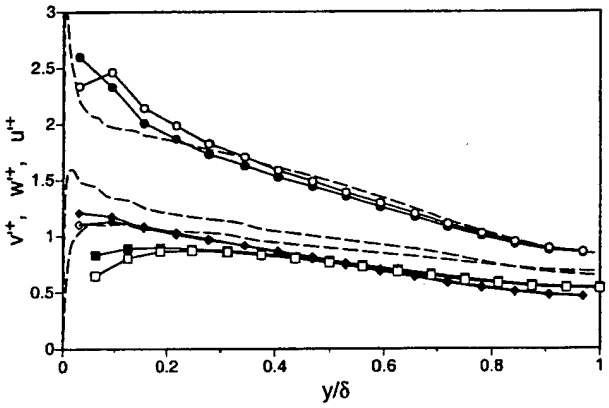

Figure 2: Resolved velocity fluctuation intensities for LES with TBLE wall stress models on a 32^3 mesh at $Re_\tau = 4000$ with (open symbols) and without (solid symbols) enhanced SGS eddy viscosity near the walls. For comparison the (unfiltered) well resolved LES data of [27] at $Re_\tau = 4000$ is shown with dashed lines.

solutions without additional time averaging.) This fix is partially justified by the consideration that the near-wall computational cells still lie well in log layer and Reynolds stresses should not be affected strongly by the presence of the wall. The improvement in the mean velocity results indicate that the under-resolved flow and inaccuracies in standard SGS models in the vicinity of walls contribute to poor predictions of dissipation and Reynolds stresses there. We note that the mixed dynamic SGS model [50], which includes a self-similar stress term, $\widetilde{\overline{\mathbf{u}}\,\overline{\mathbf{u}}} - \overline{\widetilde{\mathbf{u}}\,\widetilde{\mathbf{u}}}$, in the model for the residual stress (Eq. 7), performs worse at these coarse resolutions, because it tends to give larger residual stresses and lower eddy viscosity (dissipation), which acts entirely in the wrong direction. There is no real overall improvement in the rms velocities by enhancing the near-wall SGS eddy viscosity (Fig. 2); the shift outward in the peak of u' may indicate that the near-wall flow is just acting like a lower Reynolds number flow [6].

Another problem appears to be the development of unphysical structures near the wall. Baggett [6] showed that streak-like structures develop near the walls with maximum spanwise spacing of about 6 times the grid spacing or the physical scale, which is about 100 wall units. In moderately high Reynolds number LES the grid spacing is several hundred of wall units or greater, but the robust streak formation process causes streaks to develop with unphysically large dimensions, giving rise to unphysical velocity intensities and correlations. These structures occur in the previously presented simulations and may account in part for the inaccurate rms velocity fluctuations predicted near the walls. In this context it is interesting to note that Mason and Thomson [34] added stochastic fluctuations to the SGS model, which improved the mean velocity profiles near the walls. It is possible that the improvement occurs because the stochastic fluctuations disrupt the development of these pseudo-streaks, although this needs to be verified with more careful studies.

A notable feature about the mean streamwise velocity profiles using wall models is that they exhibit virtually no wake-like structure in the core compared with experimental data and results from better resolved simulations. This behaviour occurs for both 32^3 and 64^3 resolutions [14] and appears to be insensitive to the type of wall stress model and near-wall enhancement of the SGS eddy viscosity, even with quite vigorous wall stress fluctuations [37, 38]. A physical analogy to changing the wall conditions is the difference between smooth and rough walls. Perry et al.'s [39, 1] data show a slight drop in the wake parameter for rough walls, but nothing nearly as dramatic as seen in the coarse LES results. The lack of a wake appears instead to be due to insufficient resolution of the core flow with low-order numerical schemes. A healthy wake was recovered at $Re_\tau = 2000$ with the same numerical scheme with resolved walls [32] only when the grid spacing was about 5 times finer in the streamwise and 10 times finer in the spanwise directions than on the coarse 32^3 grid used here. This demonstrates the degree to which the second-order numerical scheme degrades the resolution of the simulation.

3.2 Separated Flow

Arnal & Friedrich [3] performed LES of flow over a step on a coarse grid using the dynamic SGS model and a law-of-the-wall wall stress model [42] on all of the solid boundaries. They found

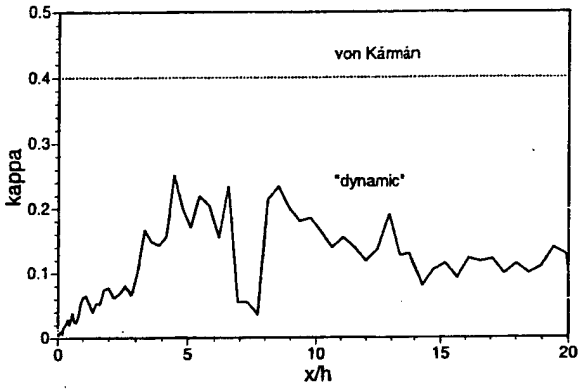

Figure 5: Instantaneous span-averaged dynamic κ in equation (2) used in the TBLE model versus its standard value of the von Kármán constant.

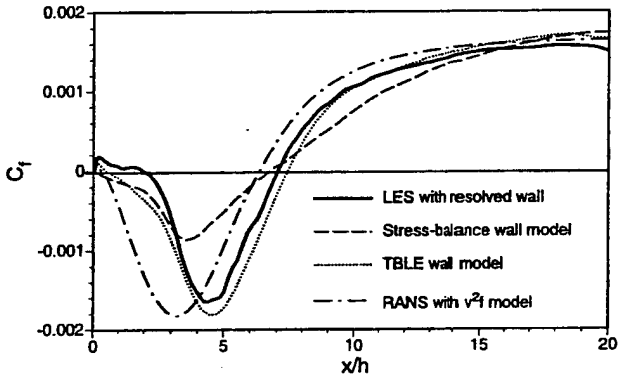

Figure 6: Friction coefficient on the bottom wall behind a step for the wall-resolved LES [2], wall stress models using stress balance and TBLE with a dynamic kappa in equation (5), and a global RANS v^2f model [18].

this correction it is found that the wall stress dips about 10% lower in the main recirculation region.

As seen in Figure 6 for the friction coefficient C_f along the bottom wall, the case using the stress balance model produces a prediction of C_f in the reverse flow that is too low by almost a factor of 2 compared with the wall-resolved calculation, and the recovery past reattachment is also seen to be too slow. When the wall stress is predicted by the thin boundary layer equations, C_f is slightly too high in the reverse flow region, but the shape of the recovery region is predicted better. The effect of C_f being slightly too high in the attached exit region may be related the problem seen in channel flow of too low a slope in the mean streamwise velocity profile near the wall, which for a fixed free stream value causes the near-wall flow to be too rapid and gives too high a value of skin friction. In both wall stress model cases, the reattachment position is in fairly good agreement with the wall-resolved LES results, as are the mean streamwise velocity profiles shown in Figure 7. On the other hand, neither of the cases captured any secondary recirculation in the corner under the step, which may not have been possible anyway on such a coarse grid. The v^2f RANS model [18],

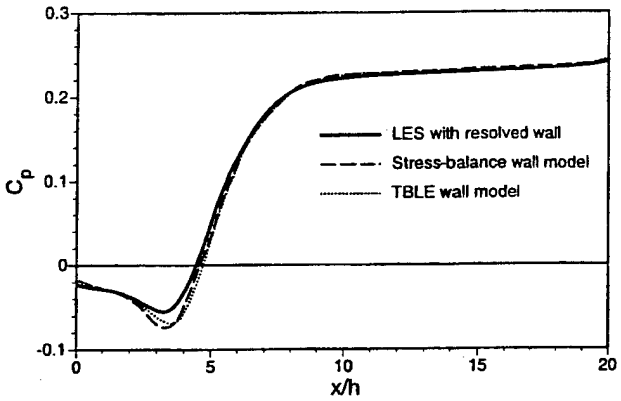

Figure 8: Pressure coefficient on the bottom wall behind a step for the wall-resolved LES [2], and stress-balance and TBLE wall stress models.

stress predictions, more appropriate models should be used, e.g., based on wall jet scaling relations (cf. [30]).

Simple stress balance models, with and without the pressure gradient, have also been applied to trailing edge flow over a hydrofoil, which features a mild separation, with fairly good results [46]. The separation point is well predicted compared with a wall-resolved LES and experimental data, although there are some discrepancies in the mean velocity profiles in the separated region. Adding the pressure gradient term to the stress balance was found to improve the skin friction results in the adverse pressure gradient region; but, as in the case of the flow behind the step, a more accurate allowance for balancing advection terms in this region is needed for further improvements.

In flow simulations of this type, the issue of providing consistent inflow conditions also arises. To avoid large transients in the inlet region, which can adversely affect results downstream and make it difficult to compare with other simulation or experimental data with any consistency, the inflow conditions should be as compatible as possible with the LES simulation, preferably computed with the same resolution, numerical scheme, and SGS and wall models. The problem also remains that the near-wall momentum predicted on coarse LES grids tends to be too high relative to the free stream, which could act to delay separation.

3.3 Model development strategies using optimal control techniques

Because there are many modelling inaccuracies near the coarsely resolved wall in addition to errors from the numerical scheme, it is not surprising that the flow develops a spurious transition zone, even if the exact wall stresses were used. Nicoud et al. [37, 38] posed the question: What wall stresses would actually be required in channel flow to obtain a good mean velocity profile? A suboptimal control strategy [10] was used to determine the wall stresses that would match a predefined log law in channel flow with $Re_\tau = 4000$ and 20000 on a very coarse grid (32^3 computational cells with a second-order finite difference scheme). The scheme was *suboptimal* in that it enforced the log law at each time step rather than in the mean.

Section 3.2. Some outer flow features, like the wake profiles in channels, require more resolution to be predicted accurately. In general there must be sufficient resolution to capture scales containing most of the energy, Reynolds shear stresses, and energy transfer. Such resolution requirements are exacerbated in low-order numerical schemes because the high wavenumbers are contaminated by dispersion errors.

There are some perhaps unavoidable discrepancies in the mean flow predictions in the first few off-wall grid points, where current subgrid-scale models are inadequate and numerical errors are large. Despite the success of wall models based on the law of the wall to predict wall stresses in some separated flow cases, improvements are still needed in the modelling of wall stresses in flows experiencing separation, reattachment, and recovery, since standard RANS models based on a law of the wall eddy viscosity are clearly invalid there. A simple "engineering" solution for general flow conditions may be to use several different scaling laws for different flow regimes, which are patched together and activated through some detection mechanism of outer flow conditions. Another solution is to apply much more sophisticated RANS models to determine the wall stresses.

One of the most glaring problems that arises is the inability to predict the near-wall subgrid-scale stresses in the outer flow reliably using standard models, including the dynamic procedure. The reasons for this are: standard SGS models are designed for isotropic flows in which the large, energy-containing scales are resolved adequately, and the physically unrealistic flow that develops on the coarse near-wall mesh cannot be used as a basis for constructing any model quantities, even dynamic coefficients, accurately. Even if accurate model stresses were supplied in the near-wall region, numerical errors from the second-order finite-differencing method degrade the effective resolution to a point where the accuracy of the first few off-wall points is degraded. Solutions for mean flow quantities throughout the near-wall region — not only wall stresses — will need to be computed from trustworthy RANS solutions matched to the core flow beyond this contaminated region. In simple flows like the channel, these quantities can be determined a posteriori. For flows with developing boundary layers or separated flow, or in other cases where the flow depends more critically on the near-wall behaviour, an iterative strategy may be required in which a RANS model, matched to long-time averages of the outer flow, is computed occasionally to correct the mean wall stresses.

Wall modelling studies are still needed using simulations with high fidelity numerical methods (e.g., spectral-spline [27]) to separate issues of numerical resolution and errors from actual wall model performance. There is also ample high Reynolds number data from turbulent pipe flow experiments for both smooth and rough walls [1, 39, 49], and it would be useful to test the performance of coarse LES in these flows using low-order finite-difference as well as higher fidelity numerical methods. We may also be able to gain some insight from the experimental data into the general effects of wall models by observing the effects of wall roughness. Ultimately, we want to incorporate wall roughness effects in an accurate way into the wall models.

The overarching question of whether wall models in LES can be considered to be successful or not at this time is rather subjective, since what is deemed acceptable depends on the flow problem at

[11] Cabot, W., Large-eddy simulations with wall models. In: *Annual Research Briefs*. Stanford: Center for Turbulence Research (1995) pp. 41–50.

[12] Cabot, W., Near-wall models in large eddy simulations of flow behind a backward-facing step. In: *Annual Research Briefs*. Stanford: Center for Turbulence Research (1996) pp. 199–210.

[13] Cabot, W., Wall models in large eddy simulation of separated flow. In: *Annual Research Briefs*. Stanford: Center for Turbulence Research (1997) pp. 97–106.

[14] Cabot, W., Jiménez, J. and Baggett, J.S., On wakes and near-wall behavior in coarse large-eddy simulation of channel flow with wall models and second-order finite-difference methods. In: *Annual Research Briefs*. Stanford: Center for Turbulence Research (1999) in press.

[15] Choi, H. and Moin, P., Effects of the computational time step on numerical simulation of turbulent flow. *J. Comp. Phys.* 113 (1994) 1–4.

[16] Dean, R.B., A single formula for the complete velocity profile in a turbulent boundary layer. *ASME J. Fluids Eng.* 98 (1976) 723–727.

[17] Deardorff, J.W., A numerical study of three-dimensional turbulent channel flow at large Reynolds numbers. *J. Fluid Mech.* 41 (1970) 453–480.

[18] Durbin, P.A., Near-wall turbulence closure without "damping functions". *Theoret. Comput. Fluid Dyn.* 3 (1991) 1–13.

[19] Germano, M., Piomelli, U., Moin, P. and Cabot, W.H., A dynamic subgrid-scale eddy viscosity model. *Phys. Fluids* 3 (1991) 1760–1765. Erratum: *Phys. Fluids* 3 (1991), 3128.

[20] Ghosal, S., An analysis of numerical errors in large-eddy simulations of turbulence. *J. Comp. Phys.* 125 (1996) 187–206.

[21] Ghosal, S. and Moin, P., The basic equations for the large eddy simulation of turbulent flows in complex geometry. *J. Comp. Phys.* 118 (1995) 24–37.

[22] Grötzbach, G., Direct numerical and large eddy simulation of turbulent channel flows. In: Cheremisinoff, N.P. (ed.), *Encyclopedia of fluid mechanics* Houston: Gulf Publ. Co. (1987) chap. 34, pp. 1337–1391.

[23] Harlow, F.H. and Welch, J.E., Numerical calculation of time-dependent viscous incompressible flow of fluid with free surface. *Phys. Fluids* 8 (1965) 2182–2189.

[24] Hoffmann, G. and Benocci, C., Approximate wall boundary conditions for large eddy simulations. In: Benzi, R. (ed.), *Advances in Turbulence V*, Dordrecht: Kluwer (1995), pp. 222–228.

[25] Kim, J. and Moin, P., Application of a fractional-step method to incompressible Navier-Stokes equations. *J. Comp. Phys.* 177 (1987) 133–166.

[41] Porté-Agel, F., Meneveau, C. and Parlange, M.B., A scale-dependent dynamic model for large-eddy simulation: application to a neutral atmospheric boundary. Submitted to *J. Fluid Mech.* (1999).

[42] Schumann, U., Subgrid scale model for finite difference simulations of turbulent flows in plane channels and annuli. *J. Comp. Phys.* 18 (1975) 376–404.

[43] Smagorinsky, J., General circulation experiments with the primitive equations. I. The basic experiment. *Mon. Weather Rev.* 91 (1963) 499–164.

[44] Sullivan, P.P., McWilliams, J.C. and Moeng, C.-H., A grid nesting method for large-eddy simulation of planetary boundary-layer flows. *Boundary-Layer Met.* 80 (1996) 167–202.

[45] Vasilyev, O.V., Lund, T.S. and Moin, P., A general class of commutative filters for LES in complex geometries. *J. Comp. Phys.* 146 (1998) 82–104.

[46] Wang, M., LES with wall model for trailing-edge aeroacoustics. In: *Annual Research Briefs.* Stanford: Center for Turbulence Research (1999) in press.

[47] Werner, H. and Wengle, H., Large-eddy simulation of turbulent flow over and around a cube in a plate channel. In: Durst, F., Friedrich, R., Launder, B.E., Schmidt, F.W., Schumann, U. and Whitelaw, J.H. (eds.) *Selected Papers from the Eighth Symposium on Turbulent Shear Flows* (1993) pp. 155–168.

[48] Wu, X. and Squires, K.D., Prediction of the three-dimensional turbulent boundary layer over a swept bump. *AIAA J.* 36 (1998) 505–514.

[49] Zagarola, M.V. and Smits, A.J., Scaling of the mean velocity profile for turbulent pipe flow. *Phys. Rev. Lett.* 78 (1997) 239–242.

[50] Zang, Y., Street, R.L. and Koseff, J.R., A dynamic mixed subgrid-scale model and its application to turbulent recirculating flows. *Phys. Fluids A* 5 (1993) 3186–3196.